METALS AND MATERIALS International, Vol. 13, No. 1 (2007), pp. 59~65

Effect of Bonding Temperatures on the Transient Liquid Phase Bonding of a Directionally Solidified Ni-based Superalloy, GTD-111

Bong Keun Lee[1,*], Woo Young Song[1], Dae Up Kim[2], In Su Woo[3], and Chung Yun Kang[1]

[1] School of Materials Science Engineering, Pusan National University, 30, Jangjeon-dong, Geumjeong-gu, Busan 609-735, Korea
[2] Hyundai MOBIS, 80-10, Mabuk-ri, Guseong-eup, Yongin-si, Gyeonggi 449-910, Korea
[3] POSCO Co. Ltd, 1, Goe-dong, Nam-gu, Pohang-si, Gyeongbuk 790-785, Korea

The bonding phenomenon and the mechanism involved in the transient liquid phase bonding (TLP Bonding) of directionally solidified Ni-based superalloy GTD-111 was investigated. At a bonding temperature of 1403 K, the liquid insert metal was eliminated by isothermal solidification, which was controlled by the diffusion of B and Si into the base metal. The solids in the bonded interlayer simultaneously grew epitaxially from the mating base metal inward from the insert metal. The number of grain boundaries formed at the bonded interlayer corresponded with those of the base metal. Liquefaction at the grain boundary and dendrite boundary occurred at a temperature of 1433 K. At a bonding temperature of 1453 K which is higher than the liquefaction temperature of the grain boundary, liquids of the insert metal were connected with liquated grain boundaries; this connection extended as far as the grain boundary, which was approximately 1.5 mm from the interface. The composition of this liquid was a mixture of the insert metal and phase that existed at the grain boundary. At extended holding times, liquid phases gradually decreased, and liquids with a continuous band shape develop into distinct islands. However, the liquid phases did not disappear after a holding period of 7.2 ks at 1453 K. The extended isothermal solidification process at the bonding temperature, which is higher than the liquefaction temperature for the grain boundary, was controlled by the diffusion of Ti. This resulted in its preferential liquefaction compared to B or Si in the insert metal.

Keywords: GTD-111, directionally solidified superalloy, transient liquid phase bonding, bonding mechanism, isothermal solidification

1. INTRODUCTION

The Ni-based superalloy GTD111 is used extensively for high temperature rotation in land-based gas turbines [1]. The degradation of engine components results from a variety of factors that include thermal cracking and distortion, oxidation, sulphidation, or other types of corrosion or erosion. In addition, fretting and wear, damage from foreign objects in the engine and distortion resulting from creep are contributing factors [2]. Rather than replacing damaged components with new ones, it more appropriate to repair the component at a cost of between 20-50 % of the cost a new component. Arc welding, EB welding, brazing and TLP bonding are frequently employed to repair these components [3]; however, the integrity of the repair ensures that the mechanical properties of the joint are close to or equivalent to the directional solidified properties of the original materials.

*Corresponding author: bklee@pusan.ac.kr

Transient Liquid Phase bonding (TLP Bonding) was examined in this study, as higher strength joints can be produced using this process compared to welding. The generally accepted reason for this is that the welding of a GTD-111 alloy can result in hot cracking and micro fissuring during fusion welding [4]. In particular, the weld metal consists of polycrystalline [5].

Transient liquid phase bonding was developed for use in joining hot cracking susceptible Ni-based cast superalloys. It is referred to as "TLP bonding" or "Activated diffusion bonding" [6]. A liquid film temporarily forms at the bonding interlayer during TLP bonding and solidifies isothermally by diffusion of a melting point depressant into the insert metal. Consequently, excellent joint quality can be expected. TLP bonding has been applied to many cast superalloys, and the mechanism of TLP bonding has been studied as well. However, the mechanism involved in the bonding of directional-solidified Ni-based superalloys in which the content of Ti is high is poorly understood.

Table 1. Chemical composition of the base metal and the insert metal used

Base Metal	Element (wt.%)													
	Cr	Co	Ti	Al	Mo	W	Ta	Fe	Mn	Si	C	Cu	B	Ni
GTD111	14.0	9.5	4.9	3.0	1.5	3.8	2.8	0.5	0.2	0.3	0.1	0.1	0.012	bal.
MBF-50	19.3	0.01	0.01	0.01	-	-	-	0.05	-	7.19	0.019	-	1.2	bal.

In this work, the change of the microstructure in joints of a directionally solidified Ni-based superalloy, GTD-111, TLP-bonded with the insert metal MBF-50 is examined as a function of the bonding temperature and holding time. The purpose of the study is to examine the phenomenon and mechanism of the bonding process as a function of the bonding temperature.

2. EXPERIMENTAL PROCEDURE

The chemical composition of the base metal and insert metal is presented in Table 1. A directionally solidified Ni-based superalloy, GTD-111, originally used as a gas turbine bucket was employed as a base metal. A thin foil of Ni-Cr-Si-B-based MBF-50 alloy was used as the filler metal. The melting range of MBF-50 is 1338-1423 K.

Specimens that were to be bonded mechanically were polished with #1500 silicon carbide paper and then cleaned by degreasing in acetone in an ultrasonic bath. The insert metal was inserted into the base metal. The bonding procedure was conducted in a high frequency induction furnace at a vacuum of 10-4 torr or greater. The specimens to be bonded were heated to 1403 and 1453 K at a rate of 4 K/s and were held at bonding temperatures for 0-7.2 ks. They were then cooled in a furnace. The pressure applied with a dead weight to the specimens was approximately 1.76 MPa. Thermocouple percussion was welded near the bonded interlayer in order to monitor the temperature.

Cross-sections of the specimens were examined with by optical microscopy, SEM, EDX, EPMA and XRD.

3. RESULT AND DISCUSSION

3.1. Bonding at 1403 K

Figure 1 shows microstructures near the interface of the joints held for various holding times at 1403 K. (a) and (b) in Fig. 2 show SEM structures of the region corresponding to the dendrite boundary (A denoted in Fig. 1) and the dendrite core (B denoted in Fig. 1) of the base metal, respectively. EDX analysis indicated that the eutectic presented in (b) in Fig. 2 consisted of a Ni-Si compound and Cr borides, and the phases shown in (c) in Fig. 2 were Cr borides. In the case of a joint held for 0 ks, a large amount of eutectic mixture that appears as a liquid at the bonding temperature was observed.

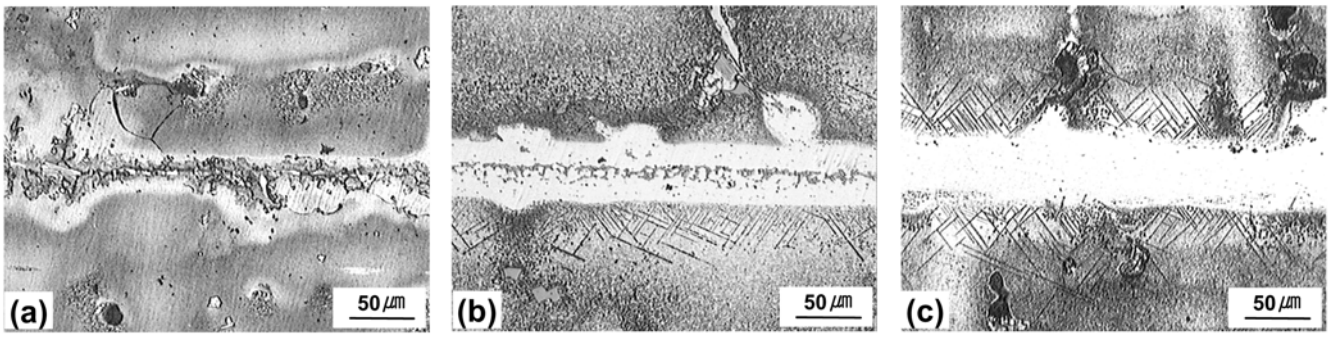

Fig. 1. Microstructures in joints bonded at 1403 K: (a) 0 ks, (b) 1.8 s, and (c) 7.2 ks.

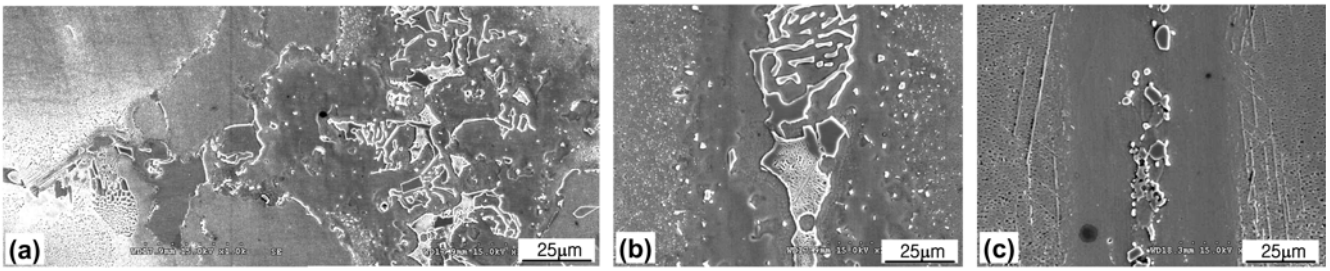

Fig. 2. SEM structures in joints bonded at 1403 K: (a) 0 ks, (b) 0 ks, and (c) 1.8 s.

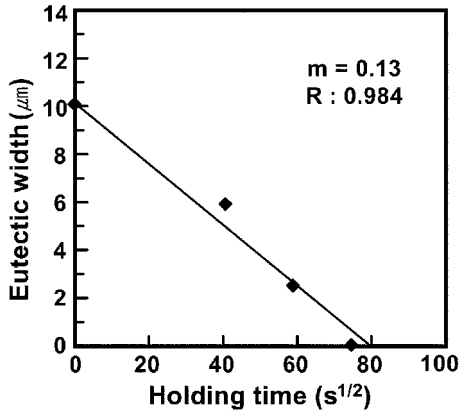

Fig. 3. The relationship between the eutectic width and the square root of the holding time at 1403 K.

Extensive formation of a eutectic mixture was discovered to have taken place along both the grain boundaries and dendrite boundaries of the base metal. This occurs because the melting points of the grain boundary and dendrite boundary regions are lower than that of the dendrite core region. As shown in Fig. 1, the amount of this eutectic mixture decreases with the holding time, and disappears after holding for 7.2 ks. From these results, it was concluded that isothermal solidification occurs at the bonded interlayer during the holding period at 1403 K.

Figure 3 shows the relationship between the eutectic width and the square root of the holding time at 1403 K. The eutectic width was determined by dividing the total area of the eutectic by the measured length, 4.5 mm. The total area of the eutectic in the bonded interlayer was examined by means of an area analyzer. A good linear correlation between the reduced eutectic width and the square root of holding time was found. These findings confirm that the isothermal solidification process at 1403 K is controlled by the diffusion of a depressant element, such as boron and silicon, into the base metal [7].

To examine the grain growth mechanism of the solid during isothermal solidification, a specimen bonded for 7.2 ks at 1403 K was used. Figure 4 shows a schematic diagram of the relationship between the grain boundary of the base metal and the grain boundary formed at the bonded interlayer. The amount of grain boundary at the bonded interlayer corresponds to the amount of both of the mating base metals.

Figure 5 shows an indexing of the EBSP pattern obtained from regions denoted as A, B and C in Fig. 4. Table 2 shows the results of an analysis of the crystallographic orientations for the transverse direction, longitudinal direction and normal direction at each position from the EBSP pattern. The crystallographic orientations for the B position in the bonded interlayer show a deviation of 1.0°-1.4° from the orientation of the base metal. As this deviation appears to be within the error range of the measurement, it can be inferred from these

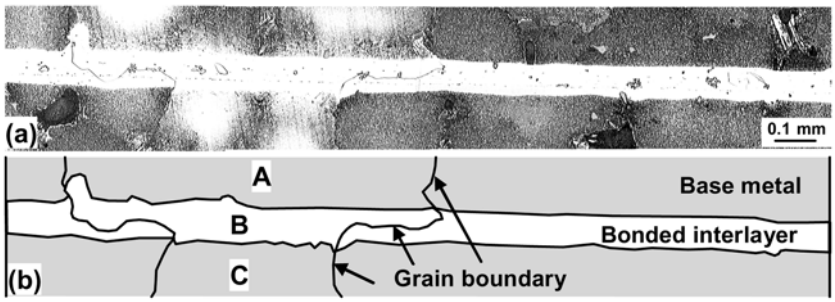

Fig. 4. The feature of grain boundary (a) formed at the bonded interlayer of a joint held at 1403 K for 3.6 ks, and its schematic diagram (b).

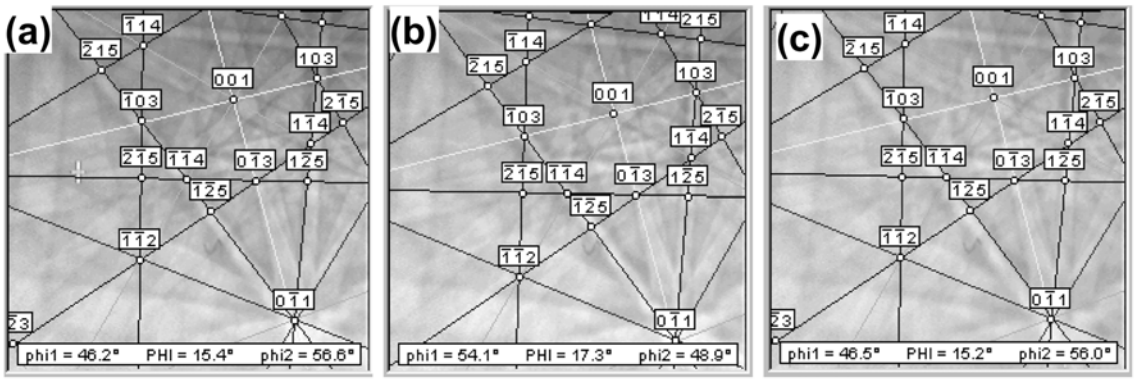

Fig. 5. The EBSP patterns obtained from regions denoted as A, B and C in Fig. 4.

Table 2. Crystallographic orientation, as analyzed from EPSP patterns

Position	Normal direction	Transverse direction	Longitudinal direction
A	92.6°	3.3°	59.4°
B	92.5°	3.1°	59.4°
C	93.4°	2.3°	57.8°

data that there is no difference between the orientation of the bonded interlayer and that of the base metal. From these results, it is clear that the solids grow epitaxially toward the liquid insert metal from both mating surfaces of the base metals during isothermal solidification.

3.2. Bonding at 1453 K

Figure 6 shows optical microstructures near the interface of joints held for various holding times at 1453 K. A clear difference between the microstructural features exhibited in Figs. 6 and 1 can be seen. At 1453 K, a significant liquid penetration at the grain boundary regions occurred, and the liquid insert metal and liquid at the grain boundary region have connected. Although, in the case of a prolonged holding (7.2 ks) time, transgranular isolated globules of the liquid phase can also be seen in the bonded interlayer and the base metal.

Figures 7 and 8 show SEM images of the results of an EPMA analysis and interpretative results for the A and B regions in (a) of Fig. 6, respectively. The liquid insert metal consists of a eutectic phase (Ni-NiSiTi), a η phase ($NiTi_3$), and CrB. The liquid insert metal for 1453 K (Fig. 7) is different from that produced at 1403 K (Fig. 2) in that a η phase is observed. This indicates that the dissolution of the base metal at 1453 K is much greater than at 1403 K. As shown in Fig. 8, the liquid at the grain boundary region also consists of the same phases formed in the liquid insert metal, but the amount of eutectic phase is less than that of the liquid insert metal. In addition, the aluminum content of the η phase in the liquid insert metal is lower than that in the grain boundary. This indicates that liquid in the bonded interlayer and liquid in the grain boundary region do not mix completely with each other.

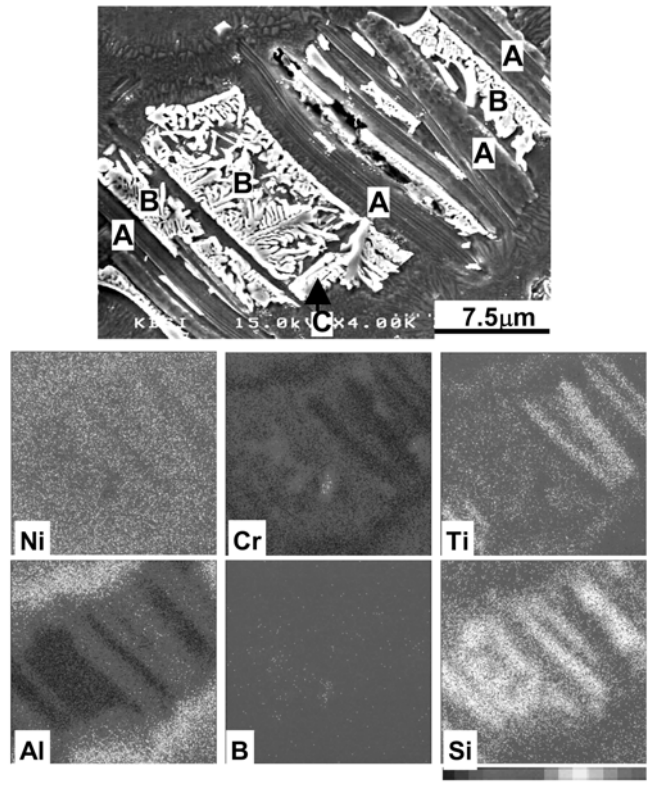

Fig. 7. SEM image and EPMA element mapping in the bonded interlayer (1453 K × 0 ks). A; η(Ni,Ti), B; NiSiTi-Ni Eutectic, C; CrB, D; Matrix.

Figure 9 shows SEM images of structures for a 18 ks holding period. The microstructure of the liquid insert metal is similar to that at the grain boundary region. As indicated in Fig. 10, the liquid insert metal also consists of the phases described above, but the extent of the eutectic phase is reduced.

A comparison of the microstructures indicates that the bonding mechanism at 1453 K is different from that at 1403 K. With this in mind, the mechanism of the bonding process at 1453 K was examined further. The maximum depth of liquid

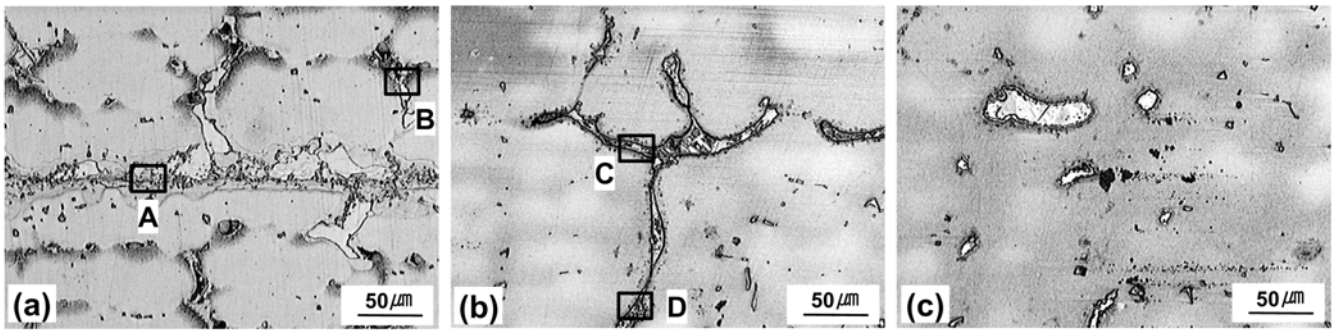

Fig. 6. Microstructures in joints bonded at 1453 K: (a) 0 ks, (b) 1.8 s, and (c) 7.2 ks.

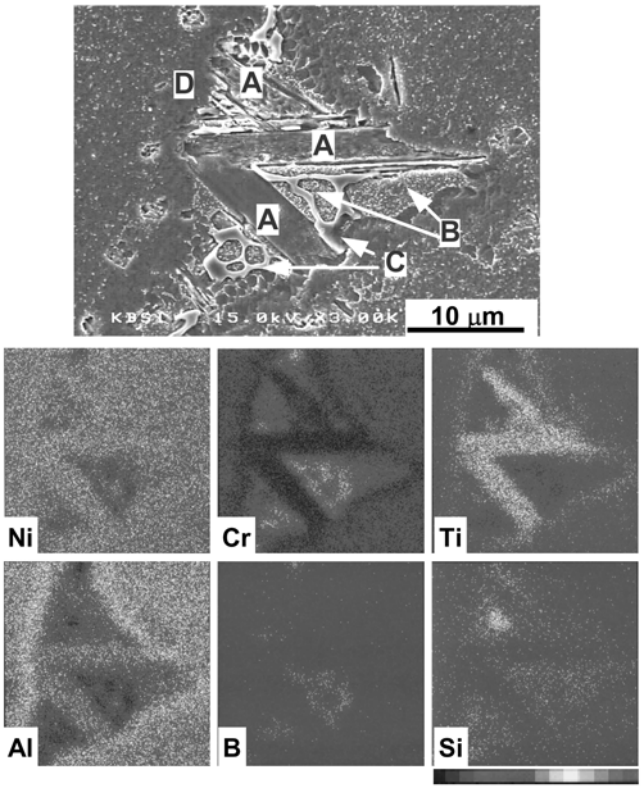

Fig. 8. SEM image and EPMA element mapping in the grain boundary region of the base metal (1453 K × 0 ks). A; η(Ni,Ti), B; NiSiTi-Ni eutectic, C; CrB, D; Matrix.

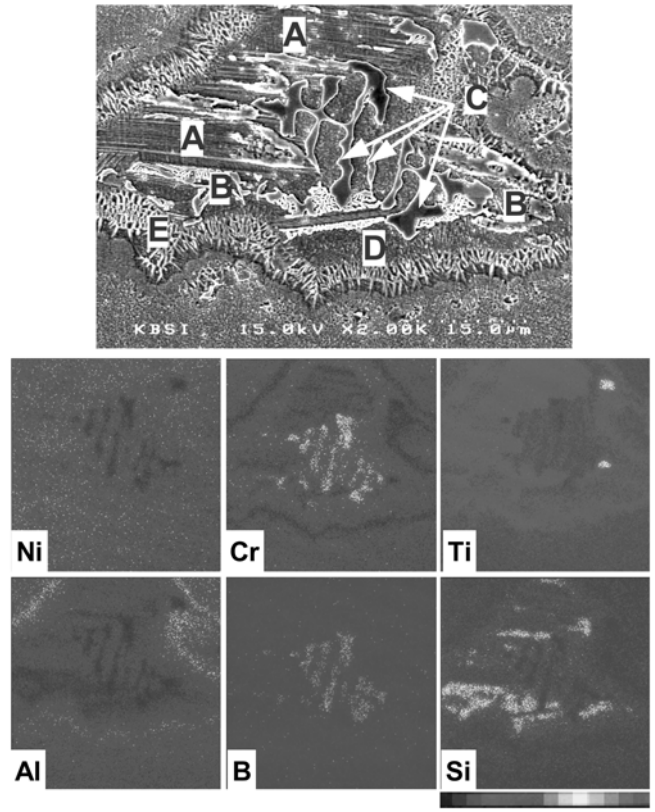

Fig. 10. SEM image and EPMA element mapping in the bonded interlayer (1453 K × 1.8 ks). A; η(Ni,Ti), B; NiSiTi-Ni Eutectic, C; CrB, D; Matrix, E: γ-γ′ eutectic.

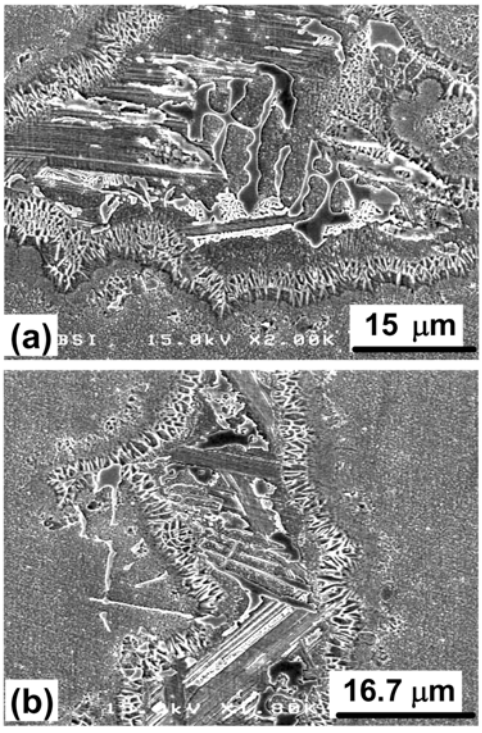

Fig. 9. SEM structures in the bonded interlayer (1453 K × 1.8 ks).

penetration at the grain boundary region was approximately 1.5 mm. Figure 11 shows the microstructures as well as the results of an EPMA analysis of a bonded joint without holding at 1473 K. (b) is observed in the bonded interlayer and (c) and (d) are observed in the grain boundary and the dendrite boundary, respectively, which is a distance of 1.5 mm from the interface. The phases in the bonded interlayer and the grain boundary contain boron and carbon, but those in the dendrite boundary contain only carbon. The presence of boron in the grain boundary some distance from the interface indicates that liquid insert metal reacted with the phases in the grain boundary, as it is impossible for this phenomenon to occur by the solid-state diffusion of boron at those bonding conditions. It is likely that this phenomenon involved liquefaction at the grain boundary.

Figure 12 shows microstructures of the base metal after heating to any temperature and then quenching. Liquefaction at the grain boundary region occurs at 1433 K. While heating and holding at a bonding temperature of 1453 K, which is above the liquefaction temperature, the insert metal melts and the grain-boundary region also undergoes liquefaction. Both liquids are then mixed. From these observations, it is clear that two types of liquids form during the bonding pro-

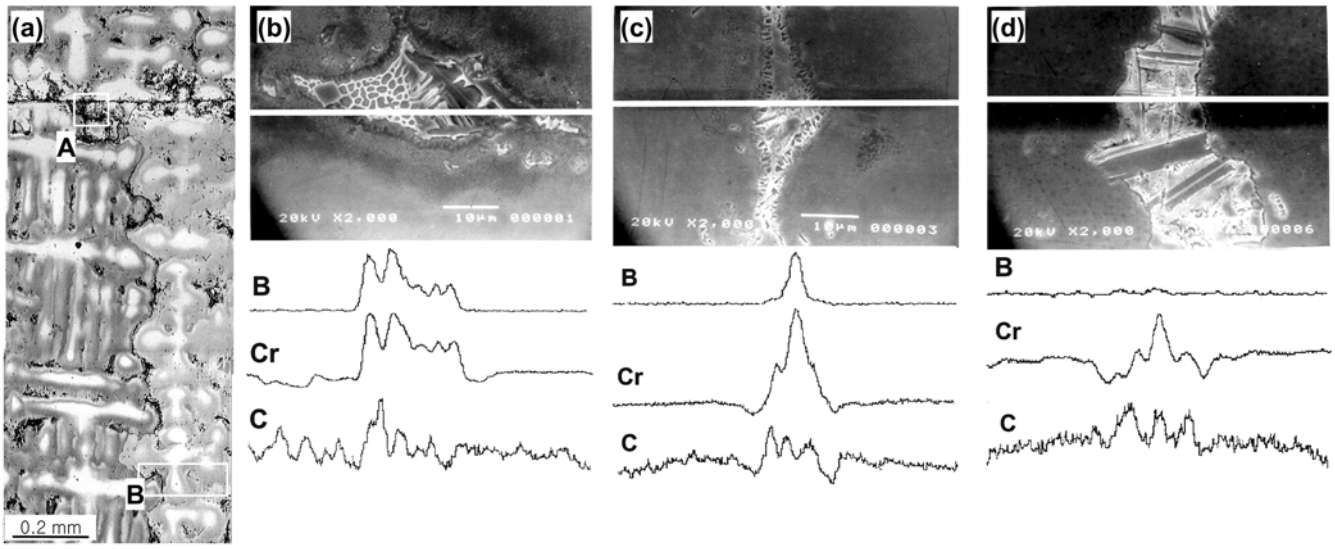

Fig. 11. Microstructures of joint bonded with holding time at 1453 Ks, and EPMA line analysis for the bonded interlayer (b), the grain boundary (c), and the dendrite boundary some distance from the interface.

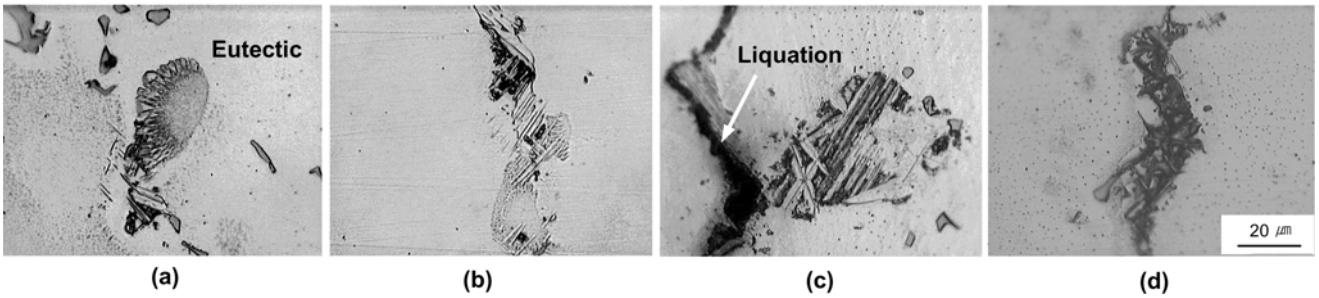

Fig. 12. Change of the microstructures at the grain boundary after water quenching at each temperature: (a) 1403 K, (b) 1423 K, (c) 1433 K, and (d) 1443 K.

cess at 1453 K. Therefore, isothermal solidification at 1453 K is controlled by the diffusion of not only boron and silicon into base metal, but titanium as well, resulting in liquid formation. Even after holding for 7.2 ks, liquids remain in the bonded interlayer, the grain boundaries and the dendrite boundaries, as the diffusion rate of titanium is slow. Therefore, it is concluded that the isothermal solidification process at 1453 K is controlled by the diffusion of titanium and not the diffusion of boron.

4. CONCLUSION

The results of this investigation are summarized below.

1. In the bonding process at 1403 K, the liquid insert metal is eliminated by the well-known mechanism of isothermal solidification, and the formation of the solid from the liquid at the interlayer occurs by epitaxial growth. In addition, the grain boundary formed at the bonded interlayer was consistent with that of the base metal.

2. In the bonding process at 1453 K, an extensive formation of the liquid phase was found to have taken place along the dendrite boundaries and grain boundaries adjacent to the bonded interlayer. Liquid phases were also observed at grain boundaries a considerable distance from the bonding interface. This phenomenon results in the liquefaction of the grain boundaries. With a prolonged holding, the liquid phases decreased gradually and changed into isolated granules, but did not completely disappear after holding for 7.2 ks at 1473 K. This isothermal solidification occurs as a result of the diffusion of Ti, resulting in liquid formation. In addition, grain boundaries formed at the bonded interlayer corresponding to those of the base metal.

3. In the TLP bonding process of the directionally solidified Ni-based superalloy GTD-111, the isothermal solidification mechanism differs with the bonding temperature.

ACKNOWLEDGMENTS

This work was supported by Grant No. 2000-1-30100-004-3 from the Basic Research Program of the Korean Science & Engineering Foundation.

REFERENCES

1. D.U. Kim and K. Nishimoto, *Met. Mater. -Int.* **8**, 403 (2002).
2. K. B. Gove, *Joining Technology*, p. 342, Metals and Materials, USA (1989).
3. K. H. Richter, *Brazing High Temperature Brazing and Diffusion Welding*, 5^{th}, p. 7-10, DVS, German (1998).
4. M. H. Haafkens, *Weld. J.* **25**, 61 (1982).
5. Nakao, *Weld. Tech.* **64**, 35 (1987).
6. W. A. Owcazarski, *Physical Metallurgy of Metal Joining,* p. 166, The Metallurgical Society of AIME, USA (1980).
7. Nakao and C.Y Kang, *J. Jpn. Weld. Soc.* **213**, 7 (1989).